ESR Studies of Heisenberg Spin Exchange. III. An ELDOR Study*

MICHAEL P. EASTMAN,† GERALD V. BRUNO,‡ AND JACK H. FREED§
Department of Chemistry, Cornell University, Ithaca, New York 14850
(Received 8 May 1969)

We report the first quantitative test of the theory for electron–electron double resonance (ELDOR) of free radicals in solution. The reduction factors R for the ELDOR spectra of aqueous solutions of the peroxylamine disulfonate dianion radical (PADS) were examined and shown to fit the theory given by Hyde, Chien, and Freed in the extrapolated limit of infinite pump power. Some of the experimental and theoretical problems are discussed. The effect of exchange on the saturation properties of PADS was investigated and shown to agree, within experimental error, with the theory discussed in Part I of this series. The implications of these results for the determination of relaxation times in complex systems are briefly discussed.

I. INTRODUCTION

An experimental study of the effects of Heisenberg spin exchange on saturation behavior in ESR spectra was described in Part I of this series.[1] The results were in agreement with the theoretical prediction that the exchange acts as though it induces simple nuclear spin–flips, which then couple all the different possible resonant transitions, and this enables a saturated transition to be relaxed via the lattice-induced electron spin–flips occurring for the other hyperfine transitions.

In Part I, the relaxation times for the narrow-line spectrum of the $TCNE^-$ radical were studied. The difficulties of measuring small changes in narrow lines, essential for exchange and saturation studies, lead to some uncertainties in the quantitative results, even though the over-all agreement with theory was good. It was felt, therefore, that a similar study should be performed on a radical with inherently broader lines, for which the concentration-independent region is easier to study. In fact the relaxation parameters $T_1(0)$ and $T_2(0)$ of the peroxylamine disulfonate dianion radical (PADS) have already been measured by Kooser, Volland, and Freed (KVF),[2] and in Part II[3] we have described its exchange behavior in considerable detail.

Our familiarity with PADS gave us an opportunity to utilize it in a quantitative test of the theory of electron–electron double resonance (ELDOR) of free radicals in liquids. In the initial study of this new technique by Hyde, Chien, and Freed (HCF),[4] most of the work was performed on a complex nitroxide radical with inhomogeneously broadened ^{14}N hyperfine lines. While the experiments and theory were in general agreement, no real attempt was made to quantitatively test the theory. This was partly because of the complications of width inhomogeneity, and also because every attempt was made to optimize signal-to-noise. This interferes with optimizing a proper quantitative analysis.

The significant potential value of ELDOR in relaxation studies was pointed out by HCF.[4] That is, the ELDOR reduction factor R depends directly on the ratio of lattice-induced nuclear spin–flip rates W_n (or ω_{HE} in the case of Heisenberg exchange) to the lattice-induced electron spin–flip rates W_e. Furthermore, a comparison of R values for different hyperfine separations of pumped and observed lines permits one to distinguish between the various types of nuclear spin–flip mechanisms such as exchange or electron–nuclear dipolar (END) interactions. The former gives effects that are independent of the number of hyperfine separations, but this is not true for the latter. The PADS system in aqueous solution is known to have a very weak END contribution to the widths,[2] so in this study a straightforward quantitative determination of the spin-exchange effects on ELDOR could be attempted.

II. EXPERIMENTAL METHODS

The PADS samples were prepared and their concentrations determined as discussed in Part II. The linewidth and saturation measurements were performed as described in Part I and by KVF. (This included corrections for modulation frequency effects as discussed by KVF.)

The ELDOR spectrometer system was similar to that described by HCF.[4,5] However, some modifications of the bimodal cavity, as described by HCF, were found to be necessary. In order to bring the frequencies of the two modes more nearly into coincidence, the length of the unshared half-wavelength portion of the (TE_{103}) mode (i.e., the top-coupled single section of the V-4534 Varian cavity) was increased by 5 mm by inserting a milled waveguide flange.

* Supported in part by the Advanced Research Projects Agency and by PHS Research Grant No. GM14123 from the National Institutes of Health.
† NIH Predoctoral Fellow 1967–1968; Gulf Oil Fellow 1966–1967. Present address: University of California, Los Alamos Scientific Laboratory, Los Alamos, N.M. 87544.
‡ NSF trainee 1965–1969.
§ Alfred P. Sloan Foundation Fellow 1966–1968.
[1] M. P. Eastman, R. G. Kooser, M. R. Das, and J. H. Freed, J.Chem. Phys. **51**, 2690 (1969). Hereafter referred to as Part I.
[2] R. G. Kooser, W. V. Volland, and J. H. Freed, J. Chem. Phys. **50**, 5243 (1969).
[3] M. P. Eastman, G. V. Bruno, and J. H. Freed, J. Chem. Phys. (to be published in 1 March issue). Hereafter referred to as Part II.
[4] J. S. Hyde, J. C. W. Chien, and J. H. Freed, J. Chem. Phys. **48**, 4211 (1968).
[5] In this work, however, a circulator replaced the magic tee in the observing arm, while in the pump arm a four-port circulator with a termination on the fourth part replaced the isolator and 3-port circulator.

Initial experiments with PADS and other charged radicals yielded spectra that were asymmetric due to a mixture of dispersion and absorption. Such effects are known to occur when a sample of high dielectric loss is located in a region of appreciable microwave E field.[2,6] We found this to be due to a misalignment of the observing (TE_{102}) mode caused by the "bulging" of this mode into the unshared portion of the cavity.[7] This bulging effect was largely removed by placing a septum at the interface of the unshared and shared cavity sections. The septum was made of highly polished silver sheet, 0.01 in. thick. Three parallel rectangular openings of 0.057×0.95 in. were cut out of the sheet. Since the large dimension of the openings was parallel to the B_p of the pump (TE_{103}) mode, the septum passed the radiation in that mode while effectively confining the observing mode to the shared portion of the cavity.

Optimum results are also dependent on sample position and on using small-diameter quartz sample tubes. The sample was positioned by moving it about in the Dewar so as to maximize the cavity "dip" on the observing klystron model. This minimizes the amount of dispersion in the detected signal. (No attempt was made to symmetrize the spectrum from the pump mode.)

It was found necessary, in order to obtain satisfactory results, to minimize the coupling of the pumping to the observing mode. This was accomplished by coupling pump power into the cavity from the pump side, then locating the Dewar in that position where the power coupled into the observing arm was a minimum. (The coupled power was measured either with a Hewlett–Packard Model 431B power meter or with the crystal detector in the observing section of the spectrometer.) The isolation of the modes with sample in place was about 45 dB when the klystron frequencies differed by about 70 MHz, and was about 40 dB for 36 MHz separation. (Higher values can be obtained for greater separations.) The coupling between modes increased appreciably as the frequency separation became less than 30 MHz, and reached less than 15 dB for separations less than 10 MHz. The procedure for achieving optimum decoupling of the modes did not depend on the use of reactive paddles (cf. HCF, Fig. 2), since these paddles appeared to lose all effectiveness whenever the coupling between the modes had been minimized carefully according to the procedure outlined.[8]

The pump klystron in these experiments had no AFC. After a 3-h warmup period, the pump klystron achieved its maximum stability with 0.02–0.03 MHz short-term fluctuations, corresponding to about 4% of the narrowest linewidth observed for the PADS solutions used in the ELDOR experiments.

The difference frequency between the pump and observing klystrons was measured with the aid of an Omni Spectra model 20816 single-ended mixer, which was fed attenuated signals from both klystrons. The output was counted using a Hewlett–Packard model 524D counter with a 525A, 10–100-MHz frequency converter unit.

In all ELDOR experiments the PADS samples were in (maximum) 1.0-mm-o.d. capillary tubes of uniform length (8.5 mm). These samples were inserted into a 2.8-mm-o.d. quartz tube, and were positioned at the same place in the cavity, as determined by the tuning procedure already described. These samples were deoxygenated, but not sealed. In most cases we could detect no significant change in widths for the duration of the ELDOR experiments. Both 15- and 100-KHz field modulation were employed during the course of the ELDOR experiments. The effective power in the observing mode was always kept well below saturation, i.e., about 4 mW incident on the cavity. (A decrease of observing power by about 10 dB had no effect on our ELDOR results.) The angle of the cavity with respect to the static magnetic field was between 20°–25°. The resonant frequency of the observing mode was about 9.05 GHz with a sample of PADS in place. The rf magnetic-field strength B_p of the pump mode is expected to vary over the sample length. For the 8.5-mm samples utilized, it was estimated from the results obtained in a standard Varian V-4531 cavity[2] that B_p^2 varies by about 30% over the length of the sample.

The following procedure was employed to obtain the optimum frequency separation between the pump and observing modes. The frequency difference between the two modes was set at the approximate PADS hyperfine splitting (73 MHz for a two hyperfine splitting, and 36.5 MHz for a one hyperfine splitting). The frequency of the pump mode was chosen to be greater than the frequency of the observing mode, because this lessened the coupling between the modes. Spectra were taken first with the pump power completely attenuated and then unattenuated. In both cases the observing signal was obtained in the usual manner by sweeping the magnetic field. A reduction factor R, defined as

$$[\text{signal amplitude (pump off)} - \text{signal amplitude (pump on)}]/\text{signal amplitude (pump off)} = R(\text{exp}),$$

could be determined. A signal amplitude was obtained as the difference in height of the derivative extrema. By varying the frequency of the pump klystron (and retuning the pump mode), it was possible to find an optimum frequency separation for which R(exp) was a maximum. This separation was considered proper for the particular sample in the cavity, and was maintained for the remainder of the experiment in which R(exp)

[6] N. Bloembergen, J. Appl. Phys. **23**, 1383 (1952).

[7] We wish to thank Mr. Robert C. Sneed of Varian Associates for helpful discussions on this matter.

[8] This was not checked at small frequency differences between the pump and observing modes. It may well be that the paddles will be of use in experiments where conditions are different from those described here.

was measured as a function of incident pump power. Although there was no AFC for the pump klystron, only slight adjustment of the reflector voltage was necessary to maintain the proper frequency separation.

In general, the separation between hyperfine lines decreases as the exchange frequency increases. Thus, the optimum frequency separation was found to depend on the PADS concentration; e.g., solutions of about $4\times10^{-2}M$ have optimum frequency separations of about 0.3 MHz (for one hyperfine splitting) to about 1.1 MHz (for two hyperfine splittings) less than those for solutions of the order of $10^{-3}M$. We were not successful, however, in our attempts to correlate the exchange frequency with the optimum frequency separation. This was mainly because of the difficulty of precisely locating the optimum separation for the broad lines of the high concentration samples (see also Sec. III).

The data for the dependence of R^{-1}(exp) on inverse pump power was obtained utilizing powers incident on the TE_{103} cavity ranging from 0.050–0.280 W, which is near maximum klystron output. The power output of the pump klystron was regularly measured using the Hewlett–Packard model 431B power meter, and it was varied with a precision variable attenuator during each run. A table of random numbers was employed to determine the order in which the power levels were run.

III. RESULTS AND ANALYSIS

A. Saturation Studies

The theoretical prediction for T_1 for the λth (degenerate) hyperfine line when the dominant relaxation terms are W_e and ω_{HE} is[1]

$$T_{1\lambda}=T_1(0)[(1+D_\lambda b'')/(1+\tfrac{1}{2}Nb'')], \quad (3.1)$$

where

$$T_1(0)=(2W_e)^{-1} \quad (3.2)$$

and is the concentration-independent value of T_1; also,

$$b''=\omega_{HE}/NW_e, \quad (3.3)$$

with N equal to the number of spin eigenstates, and D_λ is the degeneracy of the λth transition. For PADS, $N=6$ and $D_\lambda=1$ for all three lines.

For slow exchange, the Heisenberg exchange frequency ω_{HE} is related to the derivative width δ (in gauss) for PADS according to[1]

$$\omega_{HE}=(1-2D_\lambda/N)^{-1}\tfrac{1}{2}\sqrt{3}\,|\,\gamma_e\,|\,[\delta-\delta(0)]$$
$$=2.28\times10^7[\delta-\delta(0)]\ \text{sec}^{-1}, \quad (3.4)$$

where $\delta(0)$ is the concentration-independent value. It was shown in Part II that ω_{HE} is not quite a linear function of PADS concentration, so that Eq. (3.4) was used to obtain ω_{HE} directly.

The analysis based on Eqs. (3.1)–(3.4) required a knowledge of $T_1(0)$ and $T_2(0)=[\frac{1}{2}\sqrt{3}\,|\,\gamma_e\,|\,\delta(0)]^{-1}$. These values were taken from KVF who obtained $T_1(0)=T_2(0)=4.1\times10^{-7}$ sec at 24°C, where $T_1(0)$ is believed accurate to about $\pm20\%$. These results were obtained with 100 KHz field modulation, thus necessitating small modulation-frequency broadening corrections. In this work we have carefully examined the width of a $1.07\times10^{-4}M$ sample using 6 KHz modulation, and we found $T_2=(4.03\pm0.15)\times10^{-7}$ sec, which supports the earlier result.[9]

TABLE I. Relaxation times for deoxygenated and buffered solutions of PADS at 24°C.

Concentration (moles/liter)	$T_1\times10^7$ sec[a]	$T_2\times10^7$ sec[b]	b''^{-1} [c]
5.7×10^{-4}	4.11	4.11	...
6.4×10^{-3}	2.8	1.67	1.37
8.6×10^{-3}	2.0	1.33	0.956
9.8×10^{-3}	2.4	1.21	0.834
1.3×10^{-2}	1.8	0.951	0.61
1.4×10^{-2}	2.0	0.913	0.57
1.9×10^{-2}	1.6	0.646	0.37
3.5×10^{-2}	1.8	0.376	0.20
5.3×10^{-2}	1.2	0.202	0.10

[a] Error ($\pm10\%$) represents sample deviation for least-squares fit necessary in determining T_1 (cf. KVF).
[b] Error ($\pm4\%$) represents sample deviation for least-squares fit necessary in determining T_2 at near-zero incident power (cf. KVF).
[c] Based on Eqs. (3.2)–(3.4) and $T_1(0)=T_2(0)=4.1\times10^{-7}$ sec.

The use of Eqs. (3.1) and (3.2) is predicated on the assumption that there are no other nuclear-spin-dependent relaxation processes of importance. In the study of $TCNE^-$ in Part I, it was found that small but nonnegligible electron–nuclear–dipolar (END) contributions could affect the analysis. Such effects could be incorporated into Eq. (3.1) by subtracting in the numerator a term $\epsilon_\lambda=[j^D(0)/W_e][J_\lambda(J_\lambda+1)-M_\lambda^2]$, where $j^D(0)$ is the spectral density for the END mechanism. The results of KVF for PADS lead to values for ϵ of 0.0112 and 0.0056 for the central and outer lines, respectively. For our purposes this correction is negligible compared to unity.

Our results for the saturation behavior of the central component of the PADS triplet as a function of radical concentration at 24°C are given in Table I and plotted in Fig. 1. The theoretical curve was obtained from Eqs. (3.1)–(3.4), and the values for $T_1(0)$ and $T_2(0)$ were from KVF. The overall agreement is seen to be satisfactory. A quantitative assessment can be made by first rearranging Eq. (3.1) to give

$$[1-T_1/T_1(0)]=\tfrac{1}{2}b''^{-1}+\tfrac{3}{2}. \quad (3.5)$$

The experimental fit to the form of Eq. (3.5) is given in Fig. 2. The two lowest concentration points of Fig. 1

[9] Our estimate of the HE contribution to the width of these low concentration samples based on the results in Part II is 2 mG as compared to a $\delta(0)$ of 165 mG. In the work of KVF and of M. T. Jones [J. Chem. Phys. **38**, 2892 (1963)], it was found that the low-concentration PADS line shapes were not quite Lorentzian, since the lines decrease more rapidly in the wings. We have compared the shapes both at 6 and 100 kHz, and have found them to be the same within experimental error.

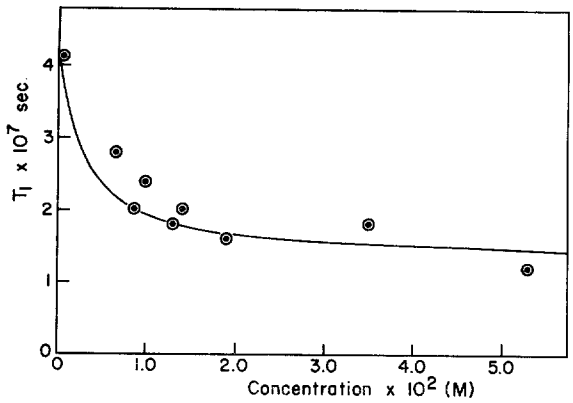

FIG. 1. T_1 as a function of concentration for aqueous PADS solutions at 24°C. The theoretical curves were determined using Eqs. (3.1)–(3-4) with $T_1(0) = 4.1 \times 10^{-7}$ sec.

were not included because their relaxation parameters lie close enough to the concentration-independent values that small errors in their values are magnified. The least-squares slope and intercept including the sample deviation are 0.8 ± 0.3 and 1.4 ± 0.2, respectively, and are thus in agreement within experimental error with the prediction of Eq. (3.5). The scatter in the experimental points of Fig. 2 is quite large. We believe this resulted, in part, from nontrivial changes in the microwave properties of the cavity when the various aqueous PADS samples were interchanged. That is, while the 1-mm (or less) PADS samples could be positioned so as to have only a small effect on the cavity Q (i.e., Q_0 values were as high as 6400), small variations from true center can yield significant changes in Q for the lossy aqueous samples. No attempts were made to correct for such variations. In view of the uncertainty in T_1 measurements in general, we note that an increased value of $T_1(0)$ by 10% to 4.5×10^{-7} sec yields a slope and intercept of 0.7 ± 0.3 and 1.4 ± 0.2, respectively, or slightly better agreement with theory.

B. ELDOR Studies

The theory for the ELDOR technique has been given by HCF for the case of nondegenerate hyperfine lines and is sufficient for an analysis of the PADS results.[4] [It can readily be extended to degenerate hyperfine lines when either ω_{HE} or when W_n (END) are the dominant nuclear-spin-flip mechanisms.][1] When the observing mode is not saturated we have

$$(Z''_{\mathrm{ESR}} - Z''_{\mathrm{ELDOR}}) \propto [d_p^2 T_p \Omega_{o,p} / (1 + \Delta\omega_p^2 T_p^2 + d_p^2 T_p \Omega_p)](1 + \Delta\omega_o^2 T_o^2)^{-1}, \tag{3.6}$$

with

$$Z''_{\mathrm{ESR}} \propto (1 + \Delta\omega_o^2 T_o^2)^{-1}, \tag{3.6'}$$

where Z''_{ESR} and Z''_{ELDOR} represent the absorption modes for ESR in the absence and presence of the pumping field, respectively, while the subscripts o and p refer to observing and pumping modes, respectively. Here $d_p^2 = \frac{1}{4}\gamma_e^2 B_p^2$, with B_p the circularly rotating component of pumping microwave magnetic field; $\Omega_p (= 4T_{1,p})$ is the saturation parameter for the pumped line, $T_p = T_{2,p}$; $\Delta\omega_p$ is the frequency deviation from resonance of the pump line. There is a similar set of terms for the observing line. The term $\Omega_{o,p}$ is the cross-saturation parameter leading to observable ELDOR effects. The theoretically predicted reduction factor R is

$$R \equiv (Z''_{\mathrm{ESR}} - Z''_{\mathrm{ELDOR}})/Z''_{\mathrm{ESR}}, \tag{3.7}$$

which yields

$$R^{-1} = \Omega_p/\Omega_{o,p} + [(1 + \Delta\omega_p^2 T_p^2)/T_p \Omega_{o,p}] d_p^{-2}. \tag{3.8}$$

Equation (3.8) is independent of the value of $\Delta\omega_o$. It appears from this equation that a plot of R^{-1} vs d_p^{-2} would give a straight line, the intercept and slope of which would yield useful relaxation information. Our experimental technique, however, involves observing derivative spectra as a result of detecting the first harmonic arising from low-amplitude field modulation. Appropriate expressions may be obtained by differentiating Eqs. (3.6) with respect to $\Delta\omega_0$, while recognizing that $\Delta\omega_p = \Delta\omega_o + \alpha$, where α represents the difference between the actual hyperfine frequency separation of observing and pumping lines and the difference in pumping and observing klystron frequencies.[10] This yields a new expression R', where

$$R'^{-1} \equiv \left(\frac{(d/d\Delta\omega_o)(Z''_{\mathrm{ESR}} - Z''_{\mathrm{ELDOR}})}{(d/d\Delta\omega_o)(Z''_{\mathrm{ESR}})} \right)^{-1}$$

$$= \frac{\Omega_p}{\Omega_{o,p}} \left[1 + \frac{d_p^{-2}}{T_p \Omega_p} \left((1 + \Delta\omega_p^2 T_p^2) - Y \frac{1 + \Delta\omega_p^2 T_p^2 + T_1 \Omega_p d_p^2}{1 + \Delta\omega_p^2 T_p^2 + T_1 \Omega_p d_p^2 + Y} \right) \right] \tag{3.9}$$

and

$$Y = (\Delta\omega_p T_p^2 / \Delta\omega_o T_o^2)(1 + \Delta\omega_o^2 T_o^2). \tag{3.9'}$$

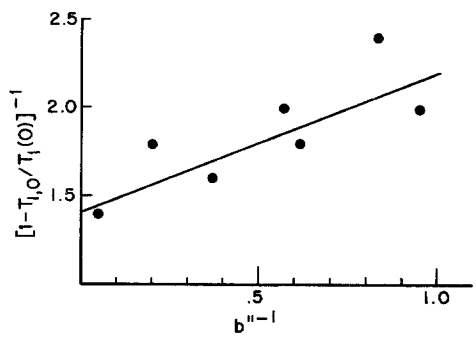

FIG. 2. Linear least-squares fit for $[1 - T_1/T_1(0)]^{-1}$ versus b''^{-1} for aqueous PADS solutions at 24°C. $T_1(0) = 4.1 \times 10^{-7}$ sec and b'' from Eqs. (3.2)–(3.4).

[10] See also J. S. Hyde, R. C. Sneed, Jr., and G. H. Rist, J. Chem. Phys. 51, 1404 (1969).

The first terms in Eq. (3.9) give the direct effect of the pumping upon the modulated (derivative) observing ESR signal, while the last term (dependent on Y) arises from the effect of modulating the pumping line upon the observing (absorption) ESR signal. For $Y=0$, the latter effect is zero, so $R'=R$. The inclusion of a finite term in Y could be expected to detract somewhat from a simple linear dependence of R'^{-1} on d_p^{-2}. It should also be noted that in our technique, both $\Delta\omega_o$ and $\Delta\omega_p$ are varied simultaneously as the observing line is swept out in order to obtain the heights of the derivative extrema. Further, there is uncertainty in each run as to whether α has been accurately set to zero. In view of these complications, as well as the inherent difficulties in measuring B_p (which varies somewhat over the sample) and the uncertain line shapes in the pumping mode (see Sec. II), it was felt that a proper analysis of the terms in d_p^{-2} of Eq. (3.9) [or (3.8)] would not be meaningful. However, the infinite power intercept

$$R_\infty'^{-1}=R_\infty^{-1}=\Omega_p/\Omega_{o,p} \tag{3.10}$$

is *independent* of all such considerations, and could therefore serve as a useful test of the ELDOR theory. We have found in all our experiments over a PADS concentration range of $5\text{–}45\times10^{-3}M$ that R^{-1} followed a linear dependence upon d_p^{-2} (or more exactly the inverse power incident on the cavity, P^{-1}), and we have extrapolated to R_∞^{-1} accordingly. These linear plots and extrapolations are shown for the different concentrations in Fig. 3. Largely as a result of the almost linear dependence of T_p on ω_{HE}, hence on concentration, the different concentration samples yielded a different degree of approach to R_∞^{-1} at the maximum pump power; the closest approach was for the more dilute samples. Nevertheless, the possibility of some departure from linearity near the intercept is not ruled out by our results.[11]

The values of R_∞^{-1} determined at the different concentrations are given in Table II[12]. This table includes

TABLE II. Values of R_∞^{-1} for ELDOR studies on aqueous PADS solutions at 24°C.

Concentration$\times10^3$ (moles/liter)	$\omega_{HE}\times10^{-6}$ sec^{-1} [a]	R_∞^{-1} [b]	b''^{-1} [c]
A. Two hyperfine separations: $\tilde{M}=1$ line observed and $\tilde{M}=-1$ line pumped			
5.5	4.97	2.50±0.09	1.47
7.2	6.87	2.42±0.09	1.07
9.5	9.73	1.89±0.24	0.752
17	14.2	1.47±0.25	0.516
28	31.4	1.40±0.15	0.233
35	37.3	1.38±0.20	0.196
45	51.0	1.16±0.40	0.144
B. One hyperfine separation: $\tilde{M}=0$ line observed and $\tilde{M}=-1$ line pumped			
4.9	4.30	2.88±0.37	1.70
6.8	6.59	2.05±0.32	1.11
15.4	13.5	1.75±0.33	0.542
16.2	14.0	1.64±0.16	0.524
17	17.9	1.50±0.19	0.410
19	20.0	1.27±0.27	0.265

[a] Calculated from Eq. (3.4).

[b] From least-squares fit of R_∞^{-1} versus P^{-1}. Error represents sample deviation least-squares intercept.

[c] Based on Eqs. (3.2)–(3.4) and $T_1(0)=T_2(0)=4.1\times10^{-7}$ sec.

one set for which the $\tilde{M}=+1$ line was observed and the $\tilde{M}=-1$ line was pumped, and another set with the $\tilde{M}=0$ line observed and the $\tilde{M}=-1$ line pumped. (Here $\tilde{M}$ is the spectral index number, cf. Part I.) The latter set, which involves the smaller separation between pump and observing frequencies, required more critical adjustment than the first. It was obtained some time after the first set, when our experimental techniques had become more precise. In Fig. 4, R_∞^{-1} is plotted versus b''^{-1} [as determined utilizing Eqs. (3.2)–(3.4)] for both sets. The linear least-squares fit to this data yields a slope and intercept of 1.03±0.08 and 1.07±0.07, respectively. This linear fit of the data is well within the experimental error in the least-squares values of the individual R_∞^{-1} as given in Table II. (The separate fit of the data for two hyperfine separations is 1.0±0.1 and 1.1±0.1 for the slope and intercept.) These results are to be compared with the theoretical values[4]:

$$\Omega_p=\Omega_o=[(1+b'')/(1+3b'')](2/W_e) \tag{3.11a}$$

and

$$\Omega_{o,p}=[b''/(1+3b'')](2/W_e) \tag{3.11b}$$

or

$$R_\infty^{-1}=1+b''^{-1}. \tag{3.12}$$

Equations 3.11 and 3.12 are independent of which pairs of lines are observed and pumped. The agreement with theory is exceptionally good, especially in view of the uncertainties in the experiment and its analysis.

IV. DISCUSSION AND CONCLUSIONS

One advantage of our saturation study on PADS as compared to our similar study on $TCNE^-$ reported in

[11] The worst deviations from linear dependence should occur in the possible case where $\Delta\omega_o=\Delta\omega_p$ over the sweep of the observing mode. Since we have $T_o=T_p\equiv T_2$, Eq. (3.9) becomes:

$$R'^{-1}=\frac{\Omega_p}{\Omega_{o,p}}\left(1+(T_p\Omega_p d_p^2)^{-1}\frac{1+\Delta\omega_o^2T_2^2}{2(1+\Delta\omega_o^2T_2^2)+T_p\Omega_p d_p^2}\right).$$

Note at the derivative extrema $(\Delta\omega_oT_2)^2=\frac{1}{3}$. One finds, however, that this equation is linear in d_p^{-2} over a very large range of $T_p\Omega_p d_p^2$; it begins to curve from linearity for $T_p\Omega_p d_p^2>2$, at which point $R'^{-1}=1.14R_\infty^{-1}$. Our results (Fig. 3) would have to be interpreted in terms of $T_p\Omega_p d_p^2<2$ in which a linear fit in d_p^{-2} (or P^{-1}) is expected, although the extrapolated intercept should be about 12% below the true value for R_∞^{-1}. While such an error would be a systematic one, it is of the order of our sample deviations from the least-squares intercepts. Crude analyses of the slopes in Fig. 3 are, however, not consistent with either simple limiting cases of $\Delta\omega_o=\Delta\omega_p$ or $Y=0$.

[12] Evaporation of a small amount of water from the PADS 8.5-mm-length samples sometimes occurred while the ELDOR spectra were taken. When this happened, the linewidths were broader by about 5%–10% after completion of the ELDOR spectra than before. In these cases the widths used in Eq. (3.4) were average widths.

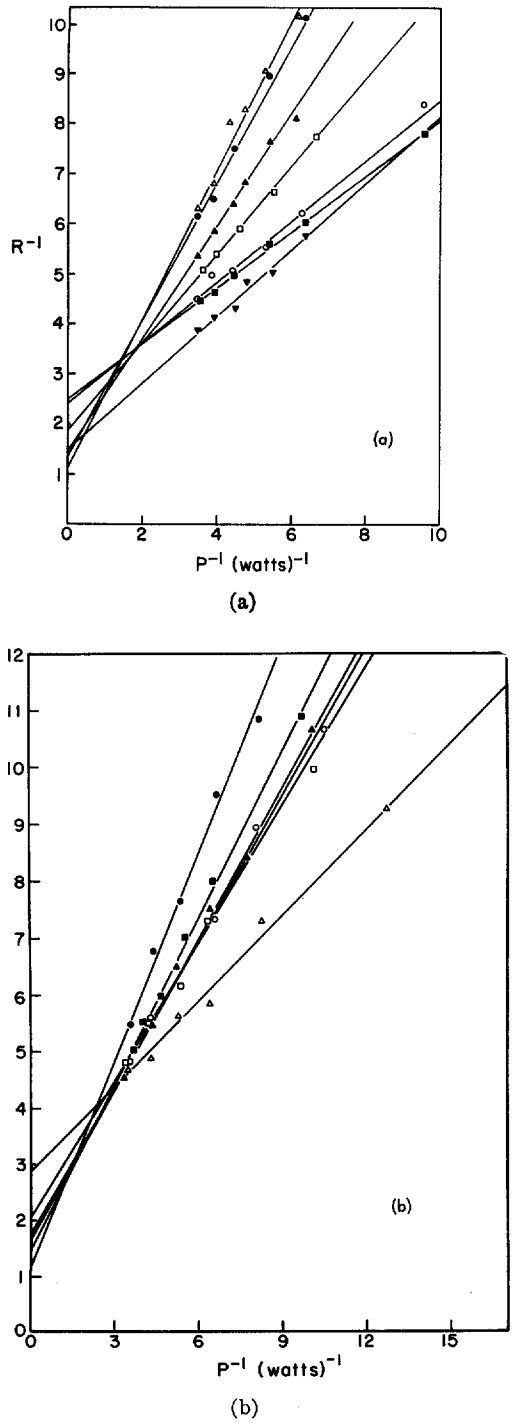

FIG. 3. Linear least-squares fit for R^{-1} versus P^{-1} (W^{-1}) for aqueous PADS solutions of different concentrations at 24°C. (a) Two hyperfine line separation ($\tilde{M}=1$ line observed and $\tilde{M}=-1$ line pumped): ■, 5.5×10^{-3} M; ○, 7.2×10^{-3} M; □, 9.5×10^{-2} M; ▼, 1.68×10^{-2} M; ▲, 2.79×10^{-2} M; ●, 3.52×10^{-2} M; △, 4.53×10^{-2} M. (b) One hyperfine line separation ($\tilde{M}=0$ line observed and $\tilde{M}=-1$ line pumped): △, 4.9×10^{-3} M; □, 6.8×10^{-3} M; ○, 1.54×10^{-2} M; ▲, 1.62×10^{-2} M; ■, 1.68×10^{-2} M; ●, 1.89×10^{-2} M.

Part I was the availability of a reasonable set of values for $T_1(0)$ and $T_2(0)$, which were obtained at moderate concentrations on lines of substantial intrinsic width. Another advantage is the insignificant contribution of END terms to the saturation behavior. These results may be taken as a further indication of the validity of the theory as outlined in Part I. However, the relative insensitivity of T_1 to ω_{HE} for moderate values of b'' is again manifested [cf. Eq. (6.3) of Part I].

Our ELDOR results for values of R_∞ (cf. Fig. 4) are quite gratifying in the quantitative agreement between theory and experiment, despite a number of uncertainties in our methods. It seems clear, then, that this technique can be very useful in extracting important information on relaxation. While in the present work all the relevant relaxation information was known

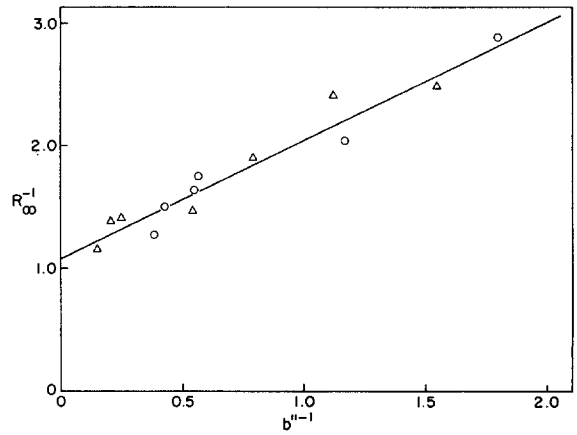

FIG. 4. Linear least-squares fit for R_∞^{-1} versus b''^{-1} for aqueous PADS solutions at 24°C. (△) represents data for two hyperfine line separation ($\tilde{M}=1$ line observed and $\tilde{M}=+1$ line pumped), while (○) represents data for one hyperfine line separation ($M=0$ line observed and $M=-1$ line pumped). The slope and intercept are 1.03 ± 0.08 and 1.07 ± 0.07, respectively, as compared to values of unity from the theoretical prediction of Eq. (3.12).

reasonably well at the outset, we can illustrate with a simple but plausible example how these techniques can be applied to a sample of unknown relaxation properties. Suppose exchange processes (Heisenberg exchange and/or chemical exchange) are the dominant nuclear-spin-dependent relaxation processes. Since both kinds of exchange are predicted to have identical relaxation effects[13] we introduce $\omega_{EX}=\omega_{HE}+\omega_{CE}$, and $b''=\omega_{EX}/NW_e$. Then Eq. (3.12), generalized for degeneracies, becomes:

$$R_\infty^{-1}-1=(D_p b'')^{-1}, \tag{4.1}$$

where D_p is the degeneracy of the pumped line. This permits a determination of b''. Then Eqs. (3.1)–(3.2) in conjunction with saturation measurements will yield W_e, so Eq. (3.3) can yield ω_{EX}. One can then determine the contributions of these terms to the width or T_2^{-1}, and the residual width, presumably due to secular con-

[13] J. H. Freed, J. Phys. Chem. **71**, 38 (1967).

tributions, (e.g., secular g-tensor and spin–rotational terms), can then be found. A study of this type, with regard to the benzene anion, will be reported on elsewhere.[14]

There are a number of ways in which the ELDOR technique can be improved for purposes of such studies. Probably the most significant would be to make use of frequency-swept ELDOR techniques[10,15] in which the field and $\Delta\omega_o$ are kept constant while $\Delta\omega_p$ is swept. This would greatly simplify the laborious tuning procedure employed in these experiments, and would help to clarify the uncertainties in the experimental analysis based on Eq. (3.9). It would also be desirable to use a more powerful pump klystron, and to improve the cavity Q of the pump mode (about 3400 in the work with the small aqueous PADS samples). This would reduce the extent of extrapolation of R^{-1} with P^{-1} in order to obtain R_∞^{-1}. Other improvements could involve stabilizing the pump klystron with an AFC and the development of techniques to reduce microwave coupling between pumping and observing modes.

[14] M. R. Das, S. B. Wagner, G. V. Bruno, and J. H. Freed, J. Chem. Phys. (to be published).
[15] J. S. Hyde, L. D. Kispert, R. C. Sneed, Jr., and J. C. W. Chien, J. Chem. Phys. **48**, 3824 (1968).

ACKNOWLEDGMENT

We wish to thank Dr. Robert G. Kooser for his considerable aid in performing the PADS saturation studies.

THE JOURNAL OF CHEMICAL PHYSICS VOLUME 52, NUMBER 1 1 JANUARY 1970

Metastable Peaks in the Mass Spectra of N_2O and NO_2. II*

AMOS S. NEWTON AND A. F. SCIAMANNA
Lawrence Radiation Laboratory, University of California, Berkeley, California 94720
(Received 23 June 1969)

Metastable peaks arising from the delayed unimolecular dissociation of NO^+ to O^++N in the mass spectra of both N_2O and NO_2 and from the dissociation of N_2^+ to N^++N in the mass spectrum of N_2O have been investigated. A new metastable dissociation of N_2O^{2+} to NO^++N^+ was also studied. Further studies were made on the previously known metastable transitions of N_2O^+ to NO^++N and of NO_2^+ to NO^++O. The appearance potential, the kinetic-energy release in fragmentation, and the half-life were determined for each metastable transition. Comparisons were made of the energetic and half-life characteristics of the metastable NO^+ ion as produced from the sources NO, N_2O, and NO_2, and of the metastable N_2^+ ion from the sources N_2 and N_2O. The results are consistent with the unimolecular dissociation of these diatomic ions, N_2^+ and NO^+, proceeding by predissociation mechanisms.

I. INTRODUCTION

Begun and Landau[1,2] reported the metastable dissociation of N_2O^+ to NO^+. This observation was later confirmed by Newton and Sciamanna,[3] and an analogous metastable dissociation of NO_2^+ to NO^+ was observed. It was further established[3] that the metastable dissociation of NO_2^+ to NO^+ proceeded from at least two excited states of NO_2^+ with the product NO^+ ions having different kinetic energies and being formed from states of different half-lives for dissociation.

Recently metastable ions in the mass spectra of N_2 and NO were observed.[4] Since N_2^+ and NO^+ are prominent fragmentation peaks in the mass spectrum of N_2O, and NO^+ is prominent in the mass spectrum of NO_2, it was of interest to examine the mass spectra of N_2O and NO_2 for the same metastable transitions previously observed in the mass spectra of N_2 and NO. The present paper presents results showing that metastable transitions of N_2^+ and NO^+ formed from N_2O, and of NO^+ formed from NO_2, do indeed occur, but with different kinetic-energy release than when formed from N_2 and NO. In addition, the metastable dissociation of N_2O^{2+} to NO^++N^+ was observed. Information on the half-lives and energetics of formation of these metastable peaks has been obtained.

II. EXPERIMENTAL

The experimental work described herein was performed using a Consolidated Electrodynamics Corporation Model 21-103B mass spectrometer. Modifications on this instrument to increase the pumping speed and ion detector sensitivity have already been described, together with the experimental methods used to investigate metastable peaks.[4,5] The present experiments were made with a collector slitwidth of 1.5 mm.

* Work performed under the auspices of the U.S. Atomic Energy Commission.
[1] G. M. Begun and L. Landau, J. Chem. Phys. **35**, 547 (1961).
[2] G. M. Begun and L. Landau, J. Chem. Phys. **36**, 1063 (1962).
[3] A. S. Newton and A. F. Sciamanna, J. Chem. Phys. **44**, 4327 (1966). This is Paper I of the series on the mass spectra of N_2O and NO_2.
[4] A. S. Newton and A. F. Sciamanna, J. Chem. Phys. **50**, 4868 (1969).
[5] A. S. Newton and A. F. Sciamanna, J. Chem. Phys. **47**, 4843 (1967).